Original Article

Synthesis, Characterization, *In-Silico* Drug Discovery And *In-Vitro* Biological Evaluation Of Morpholinium 2, 6-Pyridine Dicarboxylate

C. Anbarasi[1], P. Shanmugasundaram[2], K. Saravanan[3]*

[1, 2, 3]*Department of Chemistry, Thiruvalluvar Government Arts College, Rasipuram - 637401, India.

***Corresponding author:-** K. Saravanan

*Department of Chemistry, Thiruvalluvar Government Arts College, Rasipuram - 637401, India.
E-mail: ksaravanantgac@gmail.com; Tel: +91-9443532908
DOI:10.47750/pnr.2023.14.S01.169

Abstract

The general composition of morpholinium 2, 6-pyridine dicarboxylates are $(C_4H_{10}NO)Hdip$ (DM11), $(C_4H_{10}NO)_2dip.H_2O$ (DM12) and $(C_4H_{10}NO)Hdip.H_2dip$ (DM21), on treatment with dipicolinic acid (H2dip), the aqueous solution of morpholine yields morpholinium 2,6-pyridine dicarboxylates. The structural arrangement of the synthesized compound was confirmed by spectroscopic techniques such as FT-IR, UV, ^1H NMR and ^{13}C NMR. Infrared spectra of the salts revealed the N–H extending vibration frequencies of the nonpartisan morpholine particle in the locale 3200 - 3500 cm^{-1}. The absorption, distribution, metabolism and excretion (ADMET) properties and DFT tests were performed for the examples DM11, DM12 and DM21. The *in-vitro* calming movement was done for DM11, DM12, DM21 and Standard (diclofenac), where DM12 is taken as the norm. Atomic docking was performed for both mixtures with cyclooxygenase 1. Henceforth, our point is to discover the absorption, distribution, metabolism, excretion and toxicity (ADMET) *in-silico* model, *in-vitro* mitigating action and sub-atomic docking reads for morpholinium-inferred compounds.

Keywords: Morpholinium salts, Dipicolinates, ADMET, Anti-inflammatory activity, Molecular docking studies

1 INTRODUCTION

Morpholine is an organic chemical molecule with the formula $O(CH_2CH_2)_2NH$. Both amine and ether functional groups are present in this heterocyclic compound. Morpholine is a base because of the presence of amine, its conjugate acid is termed morpholinium. $(C_4H_{10}NO)Hdip$ (DM11), $(C_4H_{10}NO)_2dip.H_2O$ (DM12), and $(C_4H_{10}NO)Hdip.H_2dip$ (DM21)[1].

Morpholine has equivalents of Tetrahydro-1,4-oxazine; 1-Oxa-4-azacyclohexane; Diethylene oxamide [2]. The subsidiary of morpholine plays a significant part in the treatment of a variety of antimicrobial movements and insecticidal actions [3,4]. It is also utilized as an emulsifier for beauty care products, rubble waxes, cleansers and colours [5]. It has a wide scope of pharmacological properties [6], assortment of natural exercises like mitigating [7], analgesic [8], antibacterial [9], antifungal and antitumor [10,11]. Morpholinium-based cations are new to the field and a promising contender for electrochemistry, micellization and reactant applications [12-14]. Morpholinium-based cations are bipolar attributable to the concurrent presence of oxygen (electron-helpless focus) and nitrogen (electron-rich focus) [14]. The gems of the morpholinium-based mixtures with sulfosuccinate anions and long alkane chains, C8 to C18, display hexagonal columnar stages at room temperature [15]. Presently, a consistent expansion in the occurrences of irresistible infections has happened because of expanding drug opposition in microbial strains, which has become a worldwide general medical problem [16]. This issue has provoked analysts to foster new antimicrobial compounds that will be more powerful, more specific and less poisonous for battling microorganisms safely. Since many medication advancement projects come up short during clinical preliminaries because of poor absorption, distribution, metabolism and excretion (ADMET) properties, it is an astute practice to perform ADMET tests at the beginning phase of medication revelation.

DFT computational strategies are applied to investigate the frameworks to amalgamate and prepare boundaries. The cheminformatic apparatuses, including the Prediction of Activity Spectra for Substances (PASS), Lipinski's standard of five, expectations of assimilation, dissemination, digestion, discharge and harmfulness (ADMET) are helpful to understanding the compound union, natural testing and medication revelation [17-19]. Atomic docking is another cheminformatics procedure that depends on the energy scoring capacity to distinguish the most enthusiastically great ligand conformity when bound with the dynamic site of the objective [20]. The lower energy scores address better protein-ligand ties contrasted with higher energy esteems [20,21]. Hence, numerous researchers have moved their attention to discovering the molecules with calming properties that can fill in as a likely component for future medication advancement [22]. The current examination features a few patterns and properties that could be considered to plan future PPI inhibitors, either for drug disclosure tries or for synthetic science projects.

2 EXPERIMENTAL DETAILS

The metal salts, chemicals and solvents used were purchased from Merck, India and were used without further cleaning. The open capillary tube method is used to test melting points with a deep vision melting point device. The ligand and complex FT-IR spectra were acquired using the KBr pellet method on a JASCO FT/IR-4100 type A instrument. Bruker 300 MHz and 75 MHz devices were utilized to record ^{1}H and ^{13}C NMR spectra, with DMSO-d6 as the solvent and TMS as the internal reference, chemical shift values were expressed in (ppm) and coupling constants were expressed in Hz. The UV-Visible spectroscopic tests were conducted using a JASCO 007 UV-Vis spectrophotometer (V-630).

2.1 Synthesis of Morpholinium Hydrogen pyridine dicarboxylates (DM11)

1 equivalent of dipicolinic corrosive is taken in 40 ml of water. To that 1 likeness, 10% Morpholine was added to it. The pH of the solution is maintained at 6-7. The resulting solution was concentrated over a water bath and allowed for slow evaporation at room temperature. After ten days, the obtained residue was separated, washed with ice-cold water and dried. The melting point of the compound was found to be around 218-220 °C.

^{1}H NMR (400 MHz, DMSO) δ 8.22 – 8.21 (m, 1H), 8.21-8.20 (m, 2H), 3.81 – 3.80 (m, 4H), 3.15 – 3.13 (m, 4H). ^{13}C NMR (100 MHz, DMSO) δ 167.27, 149.91, 138.01, 125.14, 64.07, 43.04,

2.2 Synthesis of Dimorpholinium Pyridine dicarboxylate (DM12)

1 equivalent of dipicolinic corrosive is broken up in 40 ml of water. To that 2 likenesses, 10% Morpholine was added to it. The pH of the solution was maintained between 7-8. The resulting solution was concentrated over a water bath to one-half of its volume and allowed for slow evaporation at room temperature. After ten days, the obtained residue was collected, washed with ice-cold water and dried. The melting point of the compound was found to be around 235-237 °C.

^{1}H NMR (400 MHz, DMSO) δ 7.94 (d, *J* = 6.1 Hz, 2H), 7.84 (t, *J* = 6.4 Hz, 2H), 3.77 (brs, 8H), 3.03 (brs, 8H). ^{13}C NMR (100 MHz, DMSO) δ 169.57, 154.39, 137.58, 124.44, 64.63, 43.33.

2.3 Synthesis of Morpholinium Hydrogen pyridine dicarboxylate Pyridine dicarboxylic Acids (DM21)

2 equivalents of dipicolinic corrosive are dissolved in 40 ml of water. To that 1 likeness, 10% Morpholine was added to it. The pH of the solution is maintained between 3-5. The volume of the solution was reduced to half of its volume by heating over a water bath and allowed for slow evaporation at room temperature. The polycrystalline substances obtained were separated after a week, washed with ice-cold water and dried. The melting point of the compound was found to be around 192-194 °C.

^{1}H NMR (400 MHz, DMSO) δ 8.21 – 8.14 (m, 4H), 8.12 – 8.10 (m, 2H), 3.86 – 3.84 (m, 4H), 3.21 – 3.19 (m, 4H). ^{13}C NMR (100 MHz, DMSO) δ 167.12, 150.31, 139.24, 127.21, 64.06, 43.07,

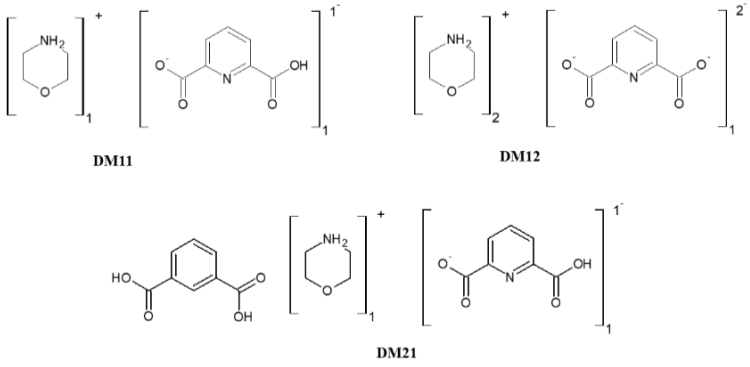

Fig. 1 Structure of Morpholinium compounds

2.4 Anti-inflammatory activity

The synthesized compounds and standard diclofenac sodium were screened for anti-inflammatory activity by using the inhibition of the albumin denaturation technique with minor modification [23, 24].
The percentage inhibition of denaturation was calculated by using the following formula.

% of Inhibition = 100 x [At - Ac /At]
At: Absorbance of test; Ac: Absorbance of control

2.5 Molecular docking studies

Atomic docking of the edifices was done with COX-1 (1PGG.pdb), and COX-2 (4COX.pdb) utilizing Hex 8.0 programming [25]. The three-dimensional designs of the metal networks were obtained utilizing Gaussian 09W

programming. The gem construction of the protein was taken from the protein data bank (www.rcsb.org). All the bounded water molecules and ligands were killed from the protein and the compound alone was utilized for docking considers.

2.6 Density Functional Theory (DFT) studies

The representation of the highest occupied molecular orbital (HOMO) and lowest unoccupied molecular orbital (LUMO) were carried out with the Gaussian 09W program, utilizing the utilitarian hypothesis [26]. The Gauss 09W programming bundle was utilized to picture the processed designs including HOMO, LUMO and Molecular electrostatic potential (MEP) portrayals.

3 RESULTS AND DISCUSSION

3.1 Infrared spectral studies

The important IR absorption bands of the acids and their salts along with the assignments are given in Table 1. The IR spectra of the ligand and its salts are shown in Fig. 2. All morpholinium salts show N-H stretching of morpholinium ion around 3060-3000 cm^{-1}, asymmetric and symmetric stretching of carboxylate 1595-1581 cm^{-1} and 1438-1359 cm^{-1}, monomorpholinium salts show the sharp intense band at 1734 and 1600 cm^{-1} due to C=O stretching of carboxylate group and free acids, dimorpholinium salt shows 1730 cm^{-1} due to C=O stretching of the carboxylate group, compound 3 (MorpHdip. H_2dip) shows a peak at 1728 cm^{-1} due to C=O stretching of carboxylate group [27]. Cleavage of the aliphatic side chains in lignin and the development of new cross-joins in lignin with build-up responses lessen the water retention properties of the samples [28,29] which increase the intensity of the peak and moved to a higher wavenumber [30-33].

Table 1. Infrared spectra for Morpholinium salts

Compound	γ_{OH}	γ_{NH}	$\gamma_{C=O}$	Assy COO^-	Sym COO^-
H_2dip	3001	-	1699	1554	1408
MorpHdip	3423	3047	1734	1595	1359
$(MorpH)_2$dip	3419	3037	1730	1587	1373
MorpHdip. H_2dip	3441	3053	1728	1581	1438

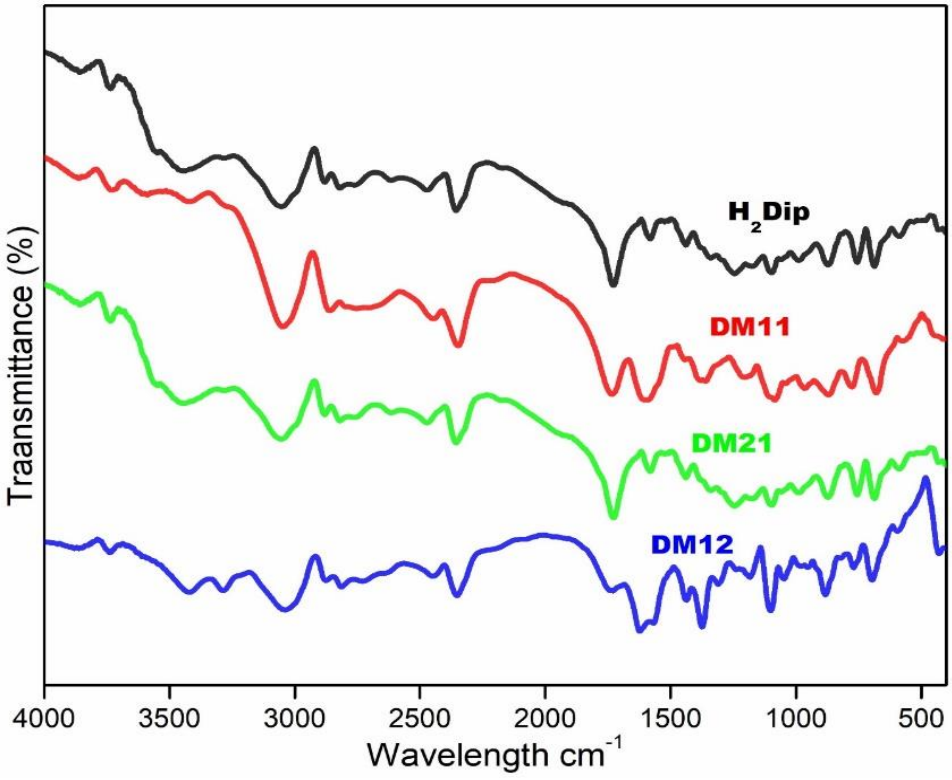

Fig. 2 IR spectra of Dipicolinic acid and Morpholinium salts

3.2 NMR spectral studies

The morpholinium 2,6-dicarboxylates was characterized using ^{1}H NMR and ^{13}C NMR spectroscopic techniques. In ^{1}H NMR, the appearance of signals around 8.22 ppm indicates the presence of C3 selective CH protons in the pyridyl unit. Similarly, the appearance of a proton signal around 8.20 ppm indicates the presence of C4 selective CH proton in the pyridyl unit. The morpholinium CH_2 signals, adjacent to oxygen appeared around 3.8 ppm. Similarly, morpholinium CH_2 signals adjacent to nitrogen appeared around 3.1 ppm. The protons count of all pyridinium carboxylates is exactly coherent in the ^{1}H NMR spectrum.

The possible carbon signals for morpholinium 2,6-dicarboxylates are 6 because the morpholinium and pyridine carboxylates are symmetric. The signals around 43 ppm appeared for morpholinium CH which is adjacent to the NH unit. Similarly, the signal around 64 ppm appeared for morpholinium CH which is adjacent to the oxygen unit. The carboxylate carbon signal appeared around 165 to 169 ppm and the C2 carbon signal of the pyridyl unit appeared around 150 ppm. The other carbon signals appeared for the remaining pyridine carbons.

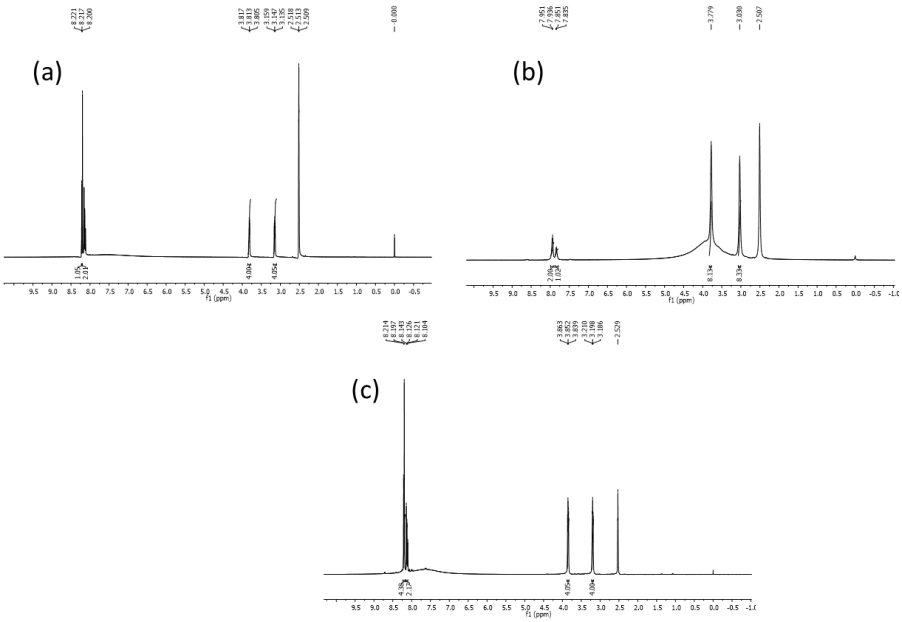

Fig .3.[1]H NMR spectrum of (a) DM11 (b) DM12 (c) DM21

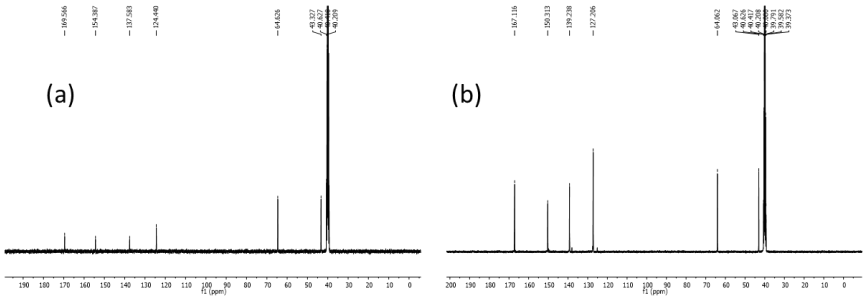

Fig.4. [13]C NMR spectrum of (a) DM12 (b) DM21

3.3 UV-Visible spectral studies

Similar concentrations of DM11, DM12, DM21 and 2,6-pyridine dicarboxylic acid (H_2dip) are dissolved in dimethyl sulfoxide and the UV-Visible spectrum is recorded. The exact absorbance variation is identified in the UV-Visible spectrum. The H_2dip showed the highest intensity and DM21 showed less absorbance than DPA because the DM21 has a 66% of pyridine dicarboxylate unit. The DM11 shows a lesser absorbance than the DM21 because the DM11 has only 50% of pyridine dicarboxylate unit. Also, the DM12 shows least absorbance due to the presence of only 33% pyridine dicarboxylate. The UV-Visible spectra for the synthesized compounds are represented in Fig. 5.

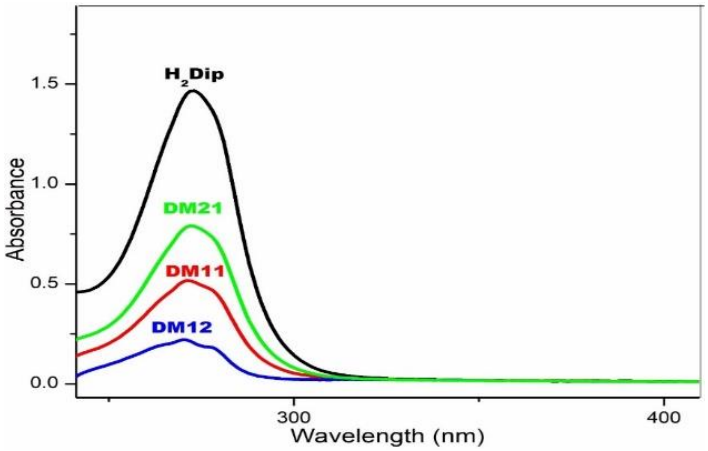

Fig.5 UV-Visible spectra of the synthesized compounds

3.4 Anti-inflammatory activity

In continuation of our endeavors to foster protected and viable calming compounds [34-36], we designed and synthesized new morpholinium hydrogen pyridine dicarboxylates (DM11), dimorpholinium pyridine dicarboxylate (DM12) and morpholinium hydrogen pyridine dicarboxylate pyridine dicarboxylic acids (DM21) hybrids are screened for in vitro anti-inflammatory activity with molecular docking studies. The anti-inflammatory profiles of the compounds are represented in Fig. 6.

The effect of DM11, DM12, DM21 and standard on heat-induced bovine serum albumin (BSA) denaturation assay was carried out by following the method used by Banuppriya et al. [24] with minor modifications. The reaction mixtures consist of varying concentrations (10, 50, 100, 250 and 500µg/mL) of DM11, DM12 and DM21 or reference drug diclofenac sodium. The results showed that 500–10 µg/mL DM11, DM12, DM21 and diclofenac sodium inhibited heat-induced BSA denaturation in a concentration-dependent manner. DM11 (239.15 µg/mL), DM12 (210.55 µg/mL), DM21 (241.34 µg/mL) significantly ($P < 0.05$) exhibited a lower inhibition of heat-induced BSA denaturation than diclofenac sodium (182.34 µg/mL). Diclofenac is a phenyl acidic corrosive subordinate and has a place in the non-steroidal mitigating drugs (NSAIDs) family [37]. Diclofenac is a strong cyclooxygenase catalyst inhibitor with complete retention and broad digestion [38]. Cell penetration is a significant component of a fiery reaction, inferable from the pivotal pretended by leukocytes [39]. During irritation, leukocytes discharge their lysosomal proteins like proteases as a component of their defensive capacities, causing extra tissue harm and ensuing aggravation [40, 41].

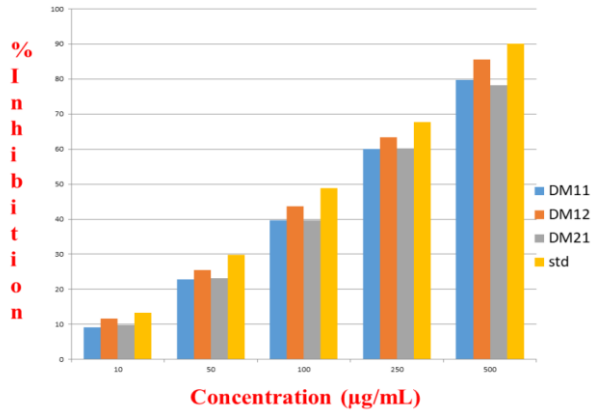

Fig. 6 Anti-inflammatory activity of (BSA denaturation technique) DM series

3.5 Drug-Likeness Prediction

The medication resemblance is directed by particle properties, including hydrophobicity, electronic circulation, hydrogen holding, atom weight, pharmacophore element, bioavailability, reactivity, harmfulness and metabolic steadiness [42]. Lipinski's rule is one of the tools most used to estimate the solubility and permeability of the compounds and thus, to predict their qualification as a drug candidates. The rule states that: poor absorption or permeation is more likely when a compound violates Lipinski rule of 5; that it has more than 5 H-bond donors (the sum of NH and OH), molecular weight (MW) is over 500, Log P is over 5 and more than 10 H-bond acceptors (the sum of N and O). The drug-likeness score for DM11 is -0.72 (Fig.7a) and for DM12 is -0.93 (Fig.7b).

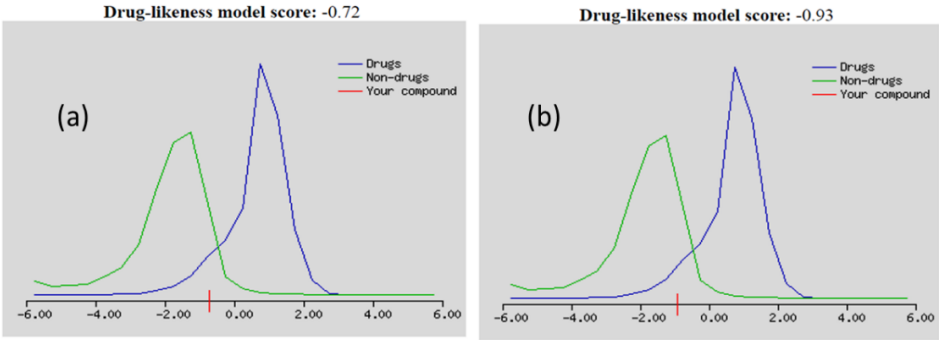

Fig. 7 Drug likeness models for (a) DM11 (b) DM12

Different between the atomic descriptors have been utilized broadly in ADMET expectation and demonstrated to be useful [43] and they can portray sub-atomic properties from various perspectives, like hydrophobicity, adaptability, H-holding capacity and so forth. It is intriguing to identify whether any of those atomic descriptors can recognize BCRP inhibitors and non-inhibitors. A few principles were created to direct the determination of mixtures in the beginning stages of medication disclosure or to plan substance compound libraries reasonable for drug revelation or synthetic science. *In-silico* pharmacokinetic has clarified in terms of ADMET and harmfulness. Further examined *in-silico* information has been associated and found in great understanding. Assessment of *in-silico* physicochemical properties or ADMET is a powerful device to affirm the capability of a medication competitor [44].

The outcomes from *In-silico* concentrates unmistakably demonstrate that the mixtures had drug-like applicant properties with no infringement of any of the medication similarity rules examined previously [40,41]. It was intriguing to take note that the consequences of the SWISS ADME indicator upsides of log [thin space (1/6-em)] P are - 0.35 and - 0.88, molar refractivity and the absolute polar surface region in these particles were in phenomenal concurrence with the main principles of medication similarity. However, these mixtures displayed a decent hydrophilic-lipophilic equilibrium and a similar anticipated bioavailability, the halogen subsidiary with high lipophilicity was relied upon to show respectable GI retention. Moreover, we determined the absolute polar surface region TPSA (A2) since it is one more key property that is identified with drug bioavailability. Hence, inactively retained atoms with TPSA >140 are thought to have low oral bioavailability, TPSA (A2) for DM11 is 85.46 and DM12 is 105.25. The outcomes got from the Swiss ADME web index are recorded in Table 2. TPSA is a boundary used to anticipate the transport properties of medications in uninvolved sub-atomic vehicles [42]. Pharmacokinetics decides the human remedial utilization of mixtures. These properties rely upon the ADMET properties [45,46], which is why *in silico* pharmacokinetics studies are important to limit the chance of disappointment of any medication in clinical preliminaries.

Table 2. *In silico* ADMET parameters important for good oral bioavailability of synthesized compounds

Compound	Abs (%)	TPSA (A^2)	MV	n-ROTB	MW	Log P	n-H-bond acceptor	n-H-bond donors	Lipinski violations
Ideal range (95% drugs)	-	<140	-	<15	<500	<5	<10	<5	<1
DM11	67.95	85.46	219.21	2	254.09	-0.35	6	3	0
DM12		105.25	301.52	2	341.16	-0.88	7	4	0

Online tools used: Molsoft and swissadme

3.6 Molecular docking studies

Sub-atomic docking is an effective method in computational science to profoundly investigate ligand acknowledgment. It has prompted significant forward leaps in drug revelation and plans in the field of restorative science. The sub-atomic docking procedure investigates the limiting mode and liking of a little particle inside the limiting site of the receptor target protein. The docked ligands were positioned by their limiting fondness in ligand-receptor buildings. Atomic docking is a significant instrument for examining the limiting affinities and ligand-target cooperation [47]; hence, we used them to study and evaluate anti-inflammatory activity. The molecular docking was performed with the most potent compound of the series DM11, DM12 and DM21. Default parameters were used for all calculations described from here on as noted in the materials and methods section. Compound DM11, DM12 and DM21 were docked at the binding sites of cyclooxygenase 1 (1PGG) and cyclooxygenase 2 (4COX) following the procedure described above.

The results of the docking studies are presented in Tables 3 and 4. The interactions with 1PGG.pdb (COX-1) and 4COX.pdb (COX-2) are shown in Fig. 8. The binding site of 1PGG is prostaglandin H2 synthase-1 complexed with 1-(4-Iodobenzoyl)-5-Methoxy-2-methylindole-3-acetic acid (Iodoindomethacin), trans model and 4COX are cyclooxygenase-2 (prostaglandin synthase-2) complexed with a non-selective inhibitor, indomethacin. In 1PGG, the binding energy (kJ mol^{-1}) for DM11 is -237.61 DM12 is 276.70 and DM21 is -323.31, where the number of hydrogen bonds in DM11 is 2, DM12 is 3 and DM21 is 1. The hydrogen bonded amino acid residues in DM11 are PRO84 (2.61Å), VAL116 (3.71Å), DM12 is TYR355 (2.42Å), TYR355 (2.20Å), TYR355 (2.18Å) and DM21 is GLU524 (2.55Å). In 4COX, the binding energy (kJ mol^{-1}) for DM11 is -230.54, DM12 is -328.91 and DM21 is -333.92Å, where the number of hydrogen bonds in DM11 is 1, DM12 is 3 and DM21 is 1. The Hydrogen bonded amino acid residues in DM11 are ARG44 (3.89Å), DM12 is TYR60 (3.07Å), GLU465 (2.31Å), ARG44 (3.03Å) and DM21 is THR118 (2.65Å). The binding energy is high in DM21 in both the binding site.

Table 3. Molecular docking metal complexes in cyclooxygenase 1 (1PGG.pdb)

S. No.	Name of the compound	Binding energy (KJ/mol)	Number of hydrogen bonding	Hydrogen bonded amino acid residues
1.	DM11	-237.61	2	PRO84 (2.61Å), VAL116 (3.71Å)
2.	DM12	-276.70	3	TYR355 (2.42Å), TYR355 (2.20Å), TYR355 (2.18Å)
3.	DM21	-323.31	1	GLU524(2.55Å)

Table 4. Molecular docking metal complexes in cyclooxygenase 2 (4COX.pdb)

S. No.	Name of the compound	Binding energy (KJ/mol)	Number of hydrogen bonding	Hydrogen bonded amino acid residues
1.	DM11	-230.54	1	ARG44 (3.89Å)
2.	DM12	-328.91	3	TYR60 (3.07Å), GLU465 (2.31Å), ARG44 (3.03Å)
3.	DM21	-333.92	1	THR118(2.65Å)

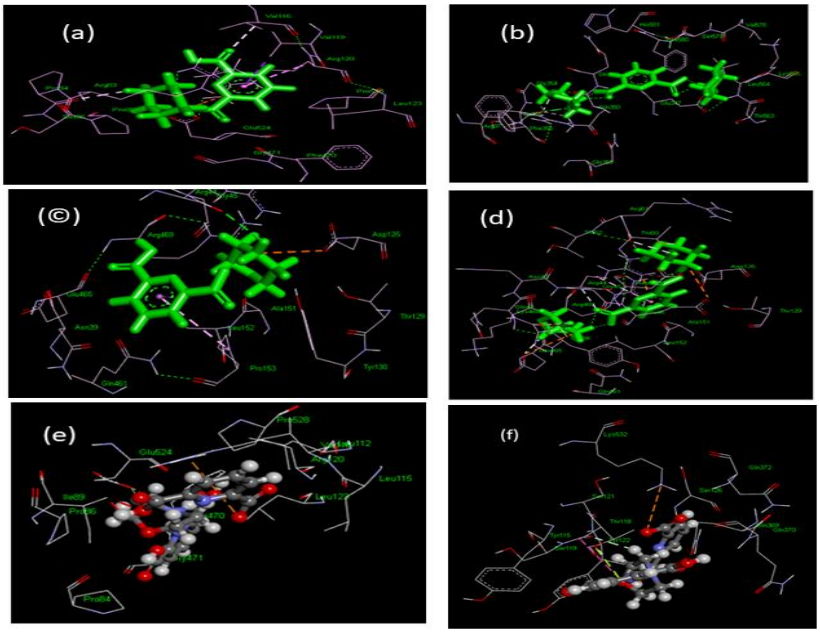

Fig. 8 Interaction of (a) DM11 with 1PGG (b) DM12 with 1PGG (c) DM11 with 4COX (d) DM12 with 4COX (e) DM21 with 1PGG (f) DM21 with 4COX

3.7 DFT studies

The density functional theory (DFT) calculations were carried out to investigate the molecular geometry and electron distribution in the compounds. Optimized geometries and molecular electrostatic potential (MEP) of the compounds were computed using density functional theory (DFT) with the basis sets. The DFT calculated Mulliken's atomic charges and revealed charge distribution in individual atoms. The HOMO, LUMO and energy gap (ΔE) of the compounds are calculated as -5.6043, -1.5782 and 4.026 for DM11, -1512, -0.2149 and 4.936 for DM12 and -3.8945,-3.5089 and 0.385 for DM21 . The DM21 showed very lower bang gap energy, the DM12 showed highest band gap energy. The outcomes uncovered that the compound DM11 showed the lesser energy hole (ΔE) than the compound DM12 proposed high synthetic reactivity and significant intermolecular charge move from the electron giver (HOMO) to the electron acceptor (LUMO) gatherings [48]. Given these outcomes, the compound DM21 has the better bioactivity contrasted than the other detailed mixtures. Furthermore, compound DM11 has higher electronegativity (χeV) and global softness (σ eV−1) contrasted with other compounds [48].

Table 4 DFT calculations of DM series

S. No	Compound name	HOMO	LUMO	The bandgap (ΔE)	Chemical potential	Global hardness	Global softness	Electrophilicity index
1.	DM11	-5.6043	-1.5782	4.026	-3.5913	2.013	0.2483	3.2035
2.	DM12	-5.1512	-0.2149	4.936	-2.6831	2.468	0.2025	1.4584
3.	DM21	-3.8945	-3.5089	0.385	-3.7017	0.1927	2.5934	35.5379

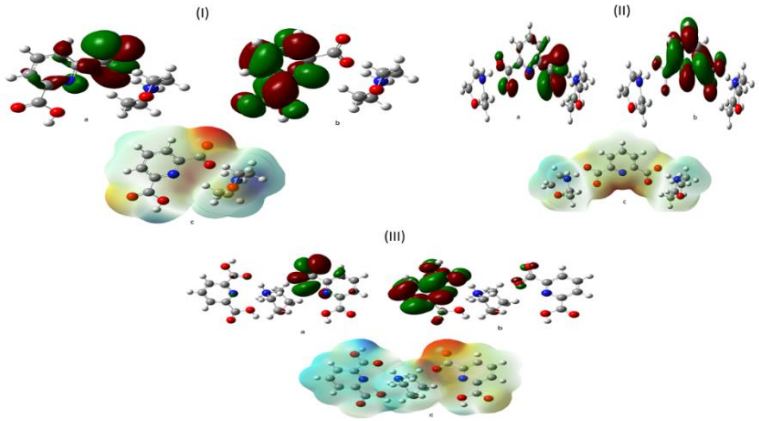

Fig. 9 Geometry optimization for (I) DM11 a) LUMO b) HOMO c) MEP (II) DM12 a) LUMO b) HOMO c) MEP (III) DM21 a) LUMO b) HOMO c) MEP

From the DFT hypothesis, a HOMO–LUMO energy partition has been determined with the particle [49]. Both orbitals show a π-type character fundamentally limited on the focal piece of the particle, which is holding at the HOMO and antibonding at the LUMO levels. The global electrophilicity list ω, communicated as μ2/2η [50], takes here the worth of

3.2035 in DM11 and 1.4584 in DM12. The electronic chemical potential μ and chemical hardness η were calculated with G03W code from the one-electron energies of the frontier orbitals. The electronic potential μ ($\mu = 1/2 \times (EHOMO + ELUMO)$ was -7.1825 eV in DM11 and -5.3661 in DM12 and the chemical hardness η ($\eta = ELUMO - EHOMO$) was 4.026 eV in DM11 and 4.936 in DM12. The maximal charge transfer ($-\mu/\eta$) is found close to unity and the nucleophilicity index N is close to 3. Based on these calculated theoretical reactivity indices, the molecule has moderate nucleophile and good electrophile characteristics.

4 CONCLUSIONS

In outline, we have arranged a bunch of morpholinium subsidiaries, DM11 morpholinium hydrogen pyridine dicarboxylates, DM12 dimorpholinium pyridine dicarboxylate and DM21 morpholinium hydrogen pyridine dicarboxylate pyridine dicarboxylic acids. The structures of newly synthesized compounds were affirmed through spectroscopic investigation. The DM12 dimorpholinium pyridine dicarboxylate showed excellent mitigating and their rate hindrance was closer to the standard. Pharmacological explanation of the mixtures was performed dependent on in-silico ADMET assessment. Due to the requests from drug revelation analysts, the improvement of *in silico* models in ADME has become more dynamic. Screening values of medication similarity results showed that all mixtures retain the pharmoclogical effect in Lipinski's standard of five. The determined boundaries HOMO and LUMO utilizing DFT estimations unmistakably upheld the docking associations. The band gap of DM12 was low. It infers that the DM12 are more responsive compounds that could be the justification for the most elevated organic movement.

DECLARATION

Ethical Approval:

This article does not contain any studies with human participants or animals performed by any of the authors.

Consent to Participate:

Not applicable

Consent to Publish:

Not applicable

Authors Contributions:

ANBARASI C: Design of the experiment and the writing of the article.
P SHANMUGASUNDARAM: Review and Editing.
K SARAVANAN: Review, editing and Supervision.

Funding:

This work was not supported by any funding agency

Competing Interests:

The authors declare that they have no conflict of interest.

Availability of data and materials:

The datasets generated during and/or analyzed during the current study are available from the corresponding author upon reasonable request.

REFERENCES

1. Chen, L. Borba, B.D. and Rohrer, J. (2013) Determination of Morpholine in Linezolid by Ion Chromatography. Thermo scientific. 1-6.
2. Pike, W. (2006) Material Safety Data Sheet Morpholine. ACS". Qorpak. 1-6.
3. Chikov, V.A.P. (2013) Morpholines. Synthesis. and biological activity. Russ. J. Org. Chem. 49(6), 787-814.
4. Kokila, N. Sarmah, N. and Patel, V.T. (2011) Synthesis, characterization, antimicrobial studies of certain s-triazine derived compounds. and analogues. Scholars research library. 3(6), 428-436.
5. Hathaway, G.J. and Proctor, N.H. (2004) Proctor. and Hughes Chemical Hazards of the Workplace. 5, 500.
6. Baluja, S. Chanda, S. Chabhadiya, R. Kachhadia, N. Nair, R. and Solanki, A.A. (2007) facile synthesis. and the antimicrobial activity of some 4-aryltriazoles J. Serb. Chem. Soc. 72(6), 539-544.
7. Sahin, D. Bayrak, H. Demirbas, A. Demirbas, N. and Karaoglu, S.A. (2012) Design. and synthesis of new 1,2,4-triazole derivatives containing morpholine moiety as antimicrobial agents , Turk J Chem. 36(3), 411-426.
8. Zaharia, V. Silvestru, A. Palibroda, N. and Mogosan, C. (2011) Synthesis. and Characterization of some bis. and Polyhetererocyclic compounds with anti-inflammatory potential. Pharmacia. 59(5), 624-635.
9. Bhat, A.M. Khan, N.S.A.S. and Mohamed, M.I. (2009) Synthesis of Triazolothiazolidinone derivatives of Coumarin with antimicrobial activity. Acta Poloniae Pharmaceutica - Drug Research. 66(6), 625-632.
10. Singh, G. Sharma, P. Dadhwal, S. Garg, P. Sharma, S. Mahajan, N. and Rawal, S. (2011) Triazoles –Impinging the Bioactivities. Int J Curr Pharm Res. 3(2), 105-118.
11. Calisir, M.M.T. Kaymakcioglu, B.K.G. Ozbek, B. and Otuk, G. (2010) Synthesis. and Antimicrobial Activity of Some Novel Schiff Bases Containing 1,2,4-Triazole-3-thione. E-Journal of Chemistry. 7(S1), 458-464.
12. Kamboj, R. Bharmoria, P. Chauhan, V. Singh, S. Kumar, A. Mithu, V.S. and Kang, T.S. (2014) Micellization Behavior of Morpholinium-Based Amide-Functionalized Ionic Liquids in Aqueous Media. Langmuir. 30, 9920-9930.
13. Brigouleix, C. Anouti, M. Jacquemin, J. Caillon-Caravanier, M. Galiano, H. and Lemordant, D. (2010) Physicochemical Characterization of Morpholinium Cation Based Protic Ionic Liquids Used as Electrolytes. Journal of Physical Chemistry B. 114, 1757-1766.

14. Yue, C.B. (2010) Aromatic Compounds Mannich Reaction Using Economical Acidic Ionic Liquids Based on Morpholinium Salts as Dual Solvent-Catalysts. Synthetic Communications. 40, 3640-3647.
15. Zhang, Q.S. Liu, A.X. Guo, B.N. and Wu, F. (2005) Synthesis of Ionic Liquids Based on the N-Methyl-NAllyl Morpholinium Cation. Chemical Journal of Chinese Universities-Chinese. 26, 340-342.
16. Lava, K. Binnemans, K. and Cardinaels, T. (2009) Piperidinium, Piperazinium. and Morpholinium Ionic Liquid Crystals. Journal of Physical Chemistry B. 113, 9506-9511.
17. Alavijeh, M.S. Chishty, M. Qaiser, M.Z. and Palmer, A.M. (2005) Drug metabolism. and pharmacokinetics, the blood-brain barrier,. and central nervous system drug discovery. NeuroRx. 2, 554–571.
18. Filimonov, D. Lagunin, A. Gloriozova, T. Rudik, A. Druzhilovskii, D. Pogodin, P. and Poroikov, V. (2014) Prediction of the biological activity spectra of organic compounds using the PASS online web resource. Chem. Heterocycl. Compd. 50, 444–457.
19. Baldi, A. (2010) Computational approaches for drug design. and discovery: An overview. Syst. Rev. Pharm. 1: 99.
20. Thomsen, R. and Christensen, M.H. (2006) MolDock: A new technique for high-accuracy molecular docking. J. Med. Chem. 49, 3315–3321.
21. Liu, Y. Xu, Z. Yang, Z. Chen, K. and Zhu, W. (2013) A knowledge-based halogen bonding scoring function for predicting protein-ligand interactions. J. Mol. Model. 19, 5015–5030.
22. Hossain, M.M. Ahamed, S.K. Dewan, S.M. Hassan, M.M. Istiaq, A. and Islam, M.S. (2014) In vivo antipyretic, antiemetic, in vitro membrane stabilization, antimicrobial,. and cytotoxic activities of different extracts from Spilanthes paniculata leaves. Biol Res. 47(1), 45.
23. Lavanya, A. Sribalan, R. and Padmini, V. (2017) Synthesis. and biological evaluation of new benzofurancarboxamide derivatives, J. Saudi Chem. Soc. 27, 277-285.
24. Banuppriya, G. Sribalan, R. and Padmini, V. (2018) Synthesis. and characterization of curcumin-sulfonamide hybrids: biological evaluation. and molecular docking studies, J. Mol. Struct. 1155, 90-100.
25. Rizvi, S.M.D. Shakil, S. and Haneef, M.A. (2013) Simple click by click protocol to perform docking: auto-dock 4.2 made easy for non-bioinformaticians, Excli J. 12, 831-857.
26. Frisch, M.J. Trucks, G.W. Schlegel, H.B. Scuseria, G.E. Robb, M.A. Cheeseman, J.R. Montgomery J.A. Jr. Vreven, T. Kudin, K.N. Burant, J.C. Millam, J.M. Iyengar, S.S. Tomasi, J. Barone, V. Mennucci, B. Cossi, M. Scalmani, G. Rega, N. Petersson, G.A. Nakatsuji, H. Hada, M. Ehara, M. Toyota, K. Fukuda, R. Hasegawa, J. Ishida, M. Nakajima, T. Honda, Y. Kitao, O. Nakai, H. Klene, M. Li, X. Knox, J.E. Hratchian, H.P. Cross, J.B. Bakken, V. Adamo, C. Jaramillo, J. Gomperts, R. Stratmann, R.E. Yazyev, O. Austin, A.J. Cammi, R. Pomelli, C. Ochterski, J.W. Ayala, P.Y. Morokuma, K. Voth, A. Salvador, P. Dannenberg, J.J. Zakrzewski, V.G. Dapprich, S. Daniels, A.D. Strain, M.C. Farkas, O. Malick, D.K. Rabuck, A.D. Raghavachari, K. Foresman, J.B. Ortiz, J.V. Cui, Q. Baboul, A.G. Clifford, S. Cioslowski, J. Tefanov, S.B.B. Liu, G. Liashenko, A. Piskorz, P. Komaromi, I. Martin, R.L. Fox, D.J. Keith, T. AlLaham, M.A. Peng, C.Y. Nanayakkara, A. Challacombe, M. Gill, P.M.W. Johnson, B. Chen, W. Wong, M.W. Gonzalez, C. Pople, J.A. Gaussian 03, Revision C.02, Gaussian, Inc. Wallingford, C.T. 2004.
27. Saravanan, K. and Govindarajan, S. (2003) Preparation. and Thermal Reactivity of Hydrazinium 2, N-Pyridinedicarboxylates (n=3, 4, 5. and 6). Journal of Thermal Analysis. and Calorimetry. 73, 951–959.
28. Boonstra, M. and Tjeerdsma, B. (2006) Chemical analysis of heat treated softwoods. European Journal of Wood. and Wood Products. 64(3), 204–211.
29. Kocaefe, D. Poncsak, S. and Boluk, Y. (2008) Effect of thermal treatment on the chemical composition. and mechanical properties of birch. and aspen. Bio Resources. 3(2), 517-537.
30. Esteves, B. Marques, A.V. Domingos, I. and Pereira, H. (2013) Chemical changes of heat treated pine. and eucalypt wood monitored by FTIR. Maderas-Cienc Tecnol. 15(2), 245-258.
31. Missio, A.L. Mattos, B.D. de Cademartori, P.H. Pertuzzatti, A. Conte, B. and Gatto, D.A. (2015) Thermochemical. and physical properties of two fast-growing eucalypt woods subjected to two-step freeze–heat treatments. Thermochimica Acta. 615, 15-22.
32. Muller, G. Schopper, C. Vos, H. Kharazipour, A. and Polle, A. (2009) FTIR-ATR spectroscopic analyses of changes in wood properties during particle-and fibreboard production of hard-and softwood trees. Bioresources. 4(1), 49-71.
33. Tjeerdsma, B. and Boonstra, M. (2006) Chemical analysis of heat treated softwoods. European Journal of Wood. and Wood Products. 64(3), 204–211.
34. Bosquesi, P.L. Melo, T.R.F. Vizioli, E.O. Dos Santos, J.L. and Chung, M.C. (2011) "Anti-inflammatory drug design using a molecular hybridization approach," Pharmaceuticals. 4(11), 1450–1474.
35. Elsaman, T. Aldeeb, O.A.A. Aboul-Fadl, T. and Hamedelneil, E.I. (2017) "Synthesis, characterization. and pharmacological evaluation of certain enzymatically cleavable NSAIDs amide prodrugs," Bioorganic Chemistry. 70, 144–152.
36. Hamid, M.H. and Elsaman, T. (2017) "A Stability-Indicating RP-HPLC-UV Method for Determination. and Chemical Hydrolysis Study of a Novel Naproxen Prodrug," Journal of Chemistry, vol. 1–10.
37. Vasilios, C.A.C. Koutakis, A. Timothy, R. Valorie, H. and Charles, R. (1988) "Jane Alissandratos. and Daniel E.Petty, Review of Diclofenac. and Evaluation of its Place in Therapy as a Nonsteroidal Antiinflammatory Agent," Drug Intelligence clinincal pharmacy. 22, 850–859.
38. Grewal, A.S. (2014) "Isatin derivatives with several biological activities," International Journal of Pharmaceutical Research. 6(1), 1–7.
39. Umapathy, E.E.J. Ndebia, A. Meeme, B. Adam, P. Menziwa, B.N. Nkeh-Chungag. and J. E. Iputo, (2010) An experimental evaluation of Albuca setosa aqueous extract on membrane stabilization, protein denaturation. and white blood cell migration during acute inflammation. Journal of Medicinal Plants Research. 4(9), 789-795.
40. Okoli Charles, O. Peter A Akah. Nkemjika J Onuoha. Theophine C Okoye. Anthonia C Nwoye. and Chukwuemeka S Nworu. (2008) Acanthus montanus: An experimental evaluation of the antimicrobial, anti-inflammatory. and immunological properties of a traditional remedy for furuncles. BMC Complementary. and Alternative Medicine. 8(1), 27.
41. Dragan, M. Stan, C.D. Panzariu, A. and Profire, L. (2016) Evaluation of anti-inflammatory potential of some new ferullic acid derivatives. Farmacia. 64(2), 194-197.
42. Ertl, P. Rohde, B. and Selzer, P. (2000) Fast calculation of molecular polar surface area as a sum of fragment-based contributions. and its application to the prediction of drug transport properties. J Med Chem. 43, 3714–3717.
43. Chen, L. Li, Y. Zhao, Q. Peng, H. and Hou, T. (2011) ADME evaluation in drug discovery. 10. Predictions of P-glycoprotein inhibitors using recursive partitioning. and Naive bayesian classifcation techniques. Mol Pharm. 8, 889–900.
44. Biswas, D. Roy, S. and Sen, S. (2006) A simple approach for indexing the oral drug likeness of a compound: discriminating drug like compounds from nondrug like ones. J Chem Inf Model. 46, 1394–1401.
45. Ekins, S. andreyev, S. Ryabov, A. Kirillov, E. Rakhmatulin, E.A. and Sorokina, S. (2006) A combined approach to drug metabolism. and toxicity assessment. Drug Metab Dispos. 34, 495–503.
46. Norinder, U. and Bergström, C.A.S. (2006) Prediction of ADMET properties. Chem Med Chem. 1, 920–937.
47. Guedes, I.A. de Magalhaes, C.S. and Dardenne, L.E. (2014) "Receptor-ligand molecular docking," Biophysical Reviews. 6(1), 75–87.
48. Abu-Melha, S. (2018) Design Synthesis and DFT/DNP modelling study of new 2-amino-5-arylazothiazole derivatives as potential antibacterial agents. Molecules. 23, 434.
49. Kandeel, M. and Kitade, Y. (2013) "Computational analysis of siRNA recognition by the Ago2 PAZ domain. and identification of the determinants of RNA-induced gene silencing," PLoS One. 8, Article ID e57140.
50. Jamroz, M.H. (2013) "Vibrational energy distribution analysis (VEDA): scopes. and limitations," Spectrochimica Acta Part A: Molecular. and Biomolecular Spectroscopy. 114, 220–230.